Angewandte Chemie
Eine Zeitschrift der Gesellschaft Deutscher Chemiker

Supporting Information

69451 Weinheim, Germany

Bidirectional Nanoparticle Crossing of Oil–Water Interfaces Induced by Different Stimuli: Insight into Phase Transfer**

Antonio Stocco, Munish Chanana, Ge Su, Peter Cernoch, Bernard P. Binks, and Dayang Wang**

anie_201203493_sm_miscellaneous_information.pdf

Supporting Information

S.1 Au@MEO_2MA_{90}-co-$OEGMA_{10}$ NP Synthesis.

Disulfide-functionalized MEO_2MA_{90}-co-$OEGMA_{10}$ polymers with molecular weight (Mw) of 25000 g/mol were synthesized via ATRP initiated with using 2,2'-dithiobis[1-(2-bromo-2-methyl-propionyloxy)ethane] $(BrC(CH_3)_2COO(CH_2)_2S)_2$.[1] This copolymer shows a lower solution temperature LCST in water around 40 °C in between the value of the two homopolymers, i.e. LCST (MEO_2MA) = 27 °C and LCST (OEGMA) = 93 °C.[2] 10 nm Au NPs were synthesized via citrate reduction of $HAuCl_4$ in water.[3] After the citrate-stabilized Au NPs and the MEO_2MA_{90}-co-$OEGMA_{10}$ polymers were incubated overnight. In order to completely remove free polymers, the aqueous dispersions of the resulting Au@MEO_2MA_{90}-co-$OEGMA_{10}$ were purified by repetition of the cycle of centrifugation, decanting supernatant, and redispersion in water till the surface tension of the supernatants was identical to that of pure water.

S.2 Au@MEO_2MA_{90}-co-$OEGMA_{10}$ NP in water.

In order to evaluate some determining properties of Au@MEO_2MA_{90}-co-$OEGMA_{10}$ NPs for the crossing phenomena, we investigated the solution and interfacial behaviors of MEO_2MA_{90}-co-$OEGMA_{10}$, citrate-stabilized Au NPs and Au@ MEO_2MA_{90}-co-$OEGMA_{10}$ NPs.

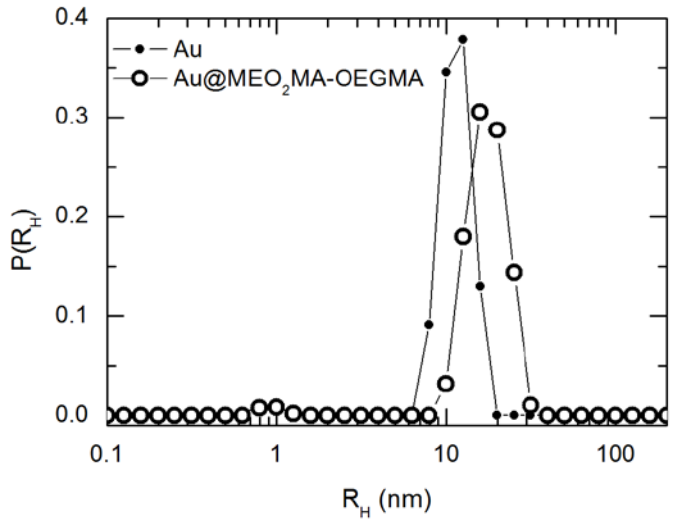

Figure S1. Distribution of hydrodynamic radius as measured by DLS for citrate-stabilized Au NPs and for the Au@MEO_2MA_{90}-co-$OEGMA_{10}$ NPs in water (concentration of NP c_{NP} = 5x10^{-2} g/L).

The hydrodynamic radius R_H (measured by dynamic light scattering (DLS)) of citrate-stabilized Au NPs was measured around 10 nm, as shown in **Fig. S1**. After the MEO_2MA_{90}-co-$OEGMA_{10}$ brushes were anchored on the NP surfaces via ligand exchange, an increase of ca. 6 nm in R_H was observed. This increase points to a polymer conformation as in a "mushroom" interfacial regime being the Flory radius $R_F = N^{3/5}\, a$ = 6 nm, considering the number of repeat units N = ca. 100 and the size of the repeating length a = 0.5 nm.

The pure copolymer MEO_2MA_{90}-co-$OEGMA_{10}$ shows a critical aggregation concentration in water around c^* = 0.1 g L^{-1} at room temperature. For $c < c^*$, a single size distribution around 4 nm was detected by DLS, with the copolymer well dissolved in water. For $c > c^*$ a second size distribution of larger aggregates appeared around 55 nm resulting from an increase in hydrophobicity. A critical temperature around 40 °C was also measured by DSC and light scattering (see **Fig. 1C**).

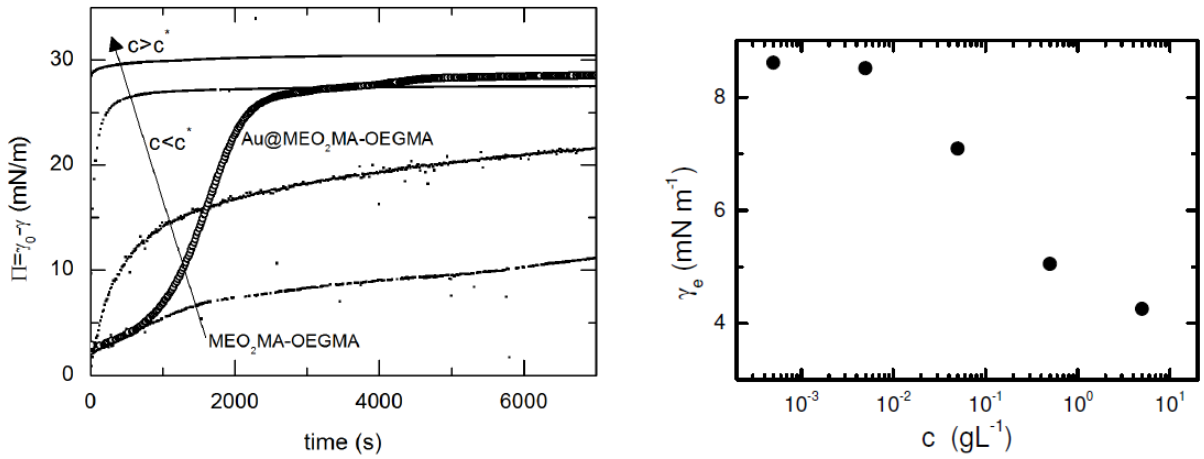

Figure S2. (Right panel) Interfacial tension measurements as a function of time at the toluene-water interface (γ_{TW} = 35 mN/m) for the pure copolymer MEO_2MA_{90}-co-$OEGMA_{10}$ (square points) at increasing concentration (c = 5 10^{-4}, 5 10^{-3}, 5 10^{-2}, 5 g/L) and for Au@MEO_2MA_{90}-co-$OEGMA_{10}$ NPs (open circles) at c_{NP} = 5 10^{-3} g/L. (Left panel) Asymphtotic interfacial tension $\gamma_e = \gamma(t\rightarrow\infty)$ values as a function of the copolymer concentration.

Some of the interfacial tension measurements as a function of time for the copolymer MEO_2MA_{90}-co-$OEGMA_{10}$ dissolved initially in water are shown in **Fig. S2**. An equilibrium interfacial tension γ_e = 4 ± 1 mN/m, (γ = 35 mN/m, experimental value) at the toluene-water interface was measured for $c > c^*$. Whilst for $c < c^*$, γ tends asymptotically to higher values, changing slowly in the time window shown in **Fig. S2**. The interfacial tension for a Au@MEO_2MA_{90}-co-$OEGMA_{10}$ NP dispersion shows a very similar plateau value (γ_e = 7 ± 1 mN/m), but with a more complex adsorption dynamics. Recently, Du et al.[4] measured the interfacial tension changes for the ligand (1-mercaptoundec-11yl)tetra(ethylene glycol) (TEG), bare Au NPs and the corresponding Au@TEG NP dispersions at oil-water interfaces. They found that bare Au NPs adsorb rapidly, reaching a low equilibrium interfacial pressure $\Pi = \gamma_0 - \gamma$ = 1 mN/m. Pure ligands being amphiphilic contributed significantly to Π, i.e. Π = 12 mN/m. For Au@TEG NP dispersions, the adsorption onto the oil-water interface was considered irreversible (Π = 14 mN/m) and presented an energy barrier ($\Delta E_B \approx 2$ kT) caused by the repulsion between NPs in the sub-phase and those adsorbed. Au@TEG and Au@MEO_2MA_{90}-co-$OEGMA_{10}$ NP dispersions present many similarities, with both systems showing complex adsorption behavior.[5]

Note that the interfacial tension for Au@MEO_2MA_{90}-co-$OEGMA_{10}$ NPs shows an additional relaxation around 4000 s, which can be interpreted as the adsorption of NPs onto an already partially covered interface. In this scenario, the interfacially trapped NPs, which are already covering the interface, need to rearrange creating some space to let other NPs, which were located into the subphase, adsorbing onto the partially crowded interface.[5]

S.3 Au@MEO_2MA_{90}-co-$OEGMA_{10}$ NP stabilized emulsions

Figure S3 shows that when the aqueous dispersions of Au@MEO_2MA_{90}-co-$OEGMA_{10}$ NPs were mixed with toluene at ionic strength in the range of 0 to 156 mM, stable emulsions were obtained after 5 min homogenization (6000 rpm). Both conductivity measurement and drop test demonstrated that the resulting emulsions were of oil-in-water type, summarized in the Table.

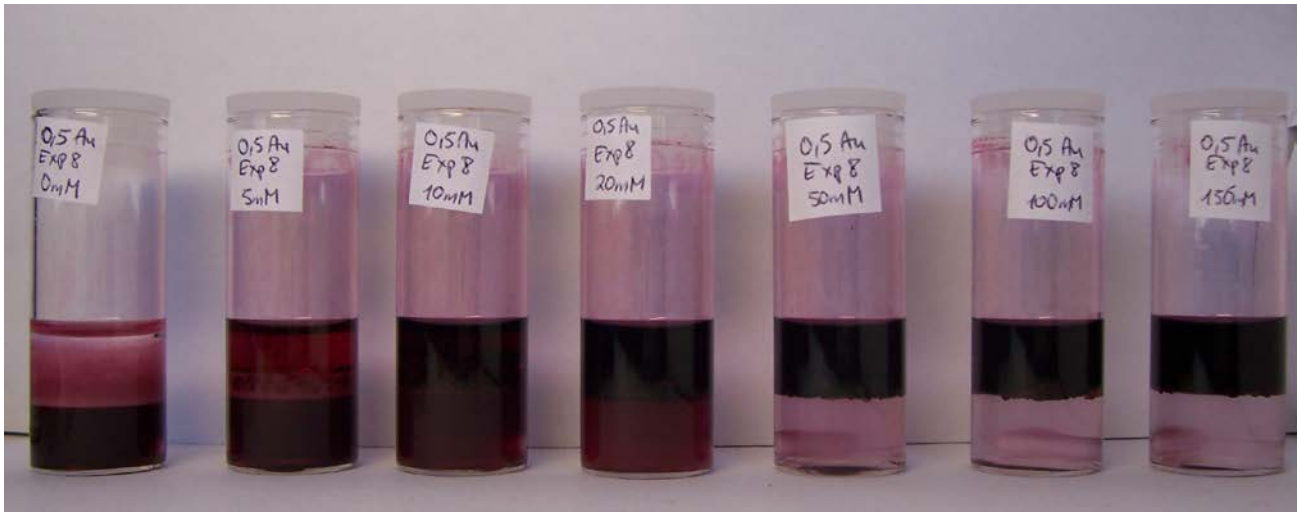

Sample (NaCl concentration labeled on glass vials)	**Conductivity**	**Drop Test in Water**	**Drop Test in Toluene**	**Emulsion Type**
0 mM	66.6 µS/cm	dispersed	sedimented	O/W
5 mM	180.7 µS/cm	dispersed	sedimented	O/W
10 mM	245 µS/cm	dispersed	sedimented	O/W
20 mM	320 µS/cm	dispersed	sedimented	O/W
50 mM	821 µS/cm	dispersed	sedimented	O/W
100 mM	1120 µS/cm	dispersed	sedimented	O/W
156 mM	1440 µS/cm	dispersed	sedimented	O/W

S4 Hexane-induced transfer of Au@MEO_2MA_{90}-co-$OEGMA_{10}$ NPs from toluene to water.

Figure S4 shows that after Au@MEO_2MA_{90}-co-$OEGMA_{10}$ NPs transferred from water to toluene upon adding salt to water, adding hexane to the toluene can induce the NP transfer back to water provided the salty water is replaced by pure water. Note that hexane is a poor solvent (precipitating agent) for MEO_2MA_{90}-co-$OEGMA_{10}$ copolymers.

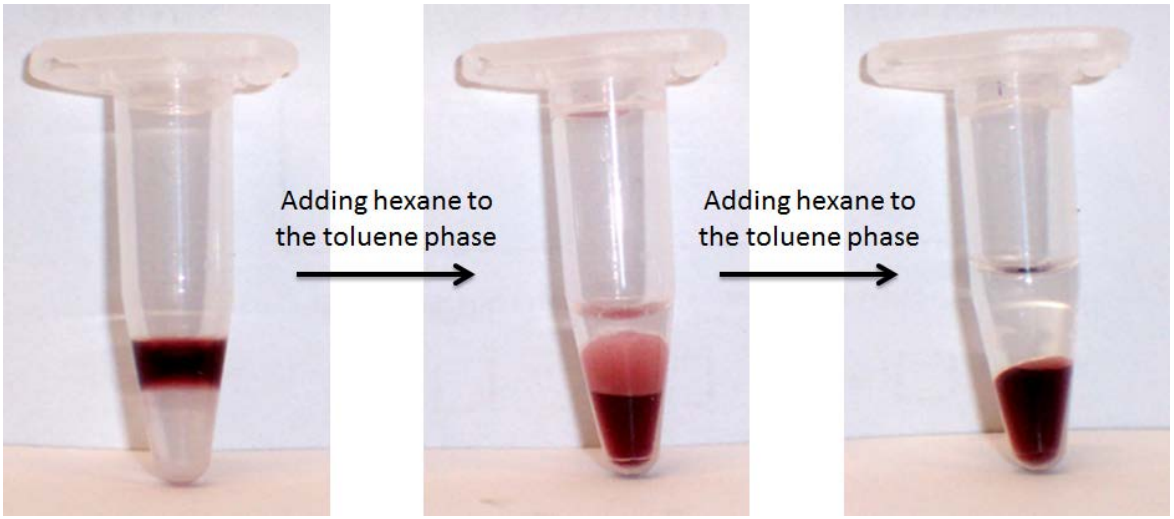

Figure S4

S.5 Free energy modeling

In the next two sections, two models to describe the free energy of a particle as a function of its position relative to the interface, i.e. $E(z)$ are presented. First, we will introduce a model for which the free energy of an isolated particle in the interfacial region between two simple liquid media can be described by the wetting energy. Then, we will present a model that accounts for the physicochemical properties of both nanoparticles and the water-toluene interface.

S.3.1. Isolated particle at an oil-water interface (ideal model)

As Pieranski described the free energy $E(z)$ of a PS colloid at the air-water interface, here we consider that in the interfacial region only the wetting energy between the nanoparticle and the media contribute to $E(z)$. Thus, $E(z) = E_W$ can be written as:[6]

$$E_W = \pi R^2 \left[2\sigma_1 \left(1 + \frac{z}{R} \right) + 2\sigma_2 \left(1 - \frac{z}{R} \right) - \gamma \left(1 - \left(\frac{z}{R} \right)^2 \right) \right] \qquad \text{(S.E1)}$$

Where R is the particle radius, z is the coordinate normal to the interface (i.e. the distance between the center of the particle and the interface: $z = 0$ at the interface and $z > 0$ in medium 1, see **Fig. 4**). σ_1, σ_2 and γ are the surface energy particle-medium 1, particle-medium 2 and the medium 1-medium 2 interfacial tension respectively. The first two terms in equation S.E1 are the energies needed to create the new interfaces and the third term is the energy gain by replacing the bare fluid interface. Note that besides the wetting no additional interactions are accounted in equation S.E1.

Figure 4 shows E_W (equation 1) for a particle of radius 10 nm at a medium 1-medium 2 interface for two specific values of surface energies (σ_1 and σ_2)[1] and three values of the medium 1-medium 2 interfacial tension ($\gamma_0 = 7$ mN/m was taken from **Fig. S2**). Comparing to the Pieranski's system (micron sized PS latex at the air-water interface), for nanometric particles at the medium 1-medium 2 interface E_W is much lower. In this model, the energy of the particle in the bulk media ($z > R$ or $z < -R$) is just the product of the area of the particle times the surface energy σ_i. Hence, in the special case when the surface energies σ_1 and σ_2 are equal (the contact angle $\theta = 90°$) this model predicts that the particle is equally wetted by either phase, i.e. there is not a thermodynamically favorable macroscopic phase for the particle. Only the interfacial region represents a favorable energetic state for a particle, showing an energy minimum at the position $z/R = (\sigma_2 - \sigma_1)/\gamma$. In **Fig. 4** for $\gamma = \gamma_0$, $\sigma_1 < \sigma_2$ and the adsorption of an isolated NP from medium 2 onto the interface is very favorable being $\Delta E = -600$ kT. Furthermore, the thermodynamic process of the transfer of a particle from phase 2 to phase 1 would be also favorable ($\Delta E = -200$ kT). The latter transfer, however, should not occur because of the high cost (ca. 400 kT) of the transfer of a NP from the interfacial region to the medium 1.

In two special cases the crossing from medium 2 to medium 1 could take place:

The first option is when the particle owns a kinetic energy, $E_K = 1/2\ m\ \langle u \rangle^2$ (where m is the mass of the particle and u is the velocity), as high as the potential well. This energy could also be provided to NPs by an external field or force (e.g. by vigorous shaking or sonication).[1, 7]

The second case is when the interface has a non-zero surface pressure. In this case $\gamma = \gamma_0 - \Pi$ and if Π is high enough, the energy minimum observed in the interfacial region could eventually vanish. This scenario could occur when surface active molecules (or NPs) are already adsorbed onto the interface. Considering equation 1 for $\sigma_1 < \sigma_2$, a critical value of $\gamma^* = \gamma_0 - \Pi^* = \sigma_2 - \sigma_1$ (see red line in **Fig.4**) can be defined (when the focus of the equation S.E1 parabola, with z/R as the independent variable, lies at z/R=1; γ^* = 0.6 mN/m in **Fig. 4**) for the vanishing of the potential well.

To summarize, in this section we describe the free energy of a particle close to the interface between two simple liquids as a function of its position. The model accounts the ideal case where only wetting energies contribute to the particle free energy in a diluted interfacial regime. The crossing phenomenon from medium 2 to medium 1 takes place when *(i)* $\sigma_1 < \sigma_2$, and *(ii)* for $\gamma = \sigma_2 - \sigma_1$ ($\sigma_2 > \sigma_1$) or when the particle is provided with an h energy high enough to escape the potential well.

S.3.2 Core@shell NP at an oil-water interface

Attempting to describe more realistically the nanoparticle crossing phenomenon, the free energy of a core@shell nanoparticle as a function of its position relative to the interface should be modeled accounting for the rich range of interactions between the core@shell nanoparticle and the interface in a semi dilute interfacial regime (NP interface coverage between 10% and 40%). Interactions between the polymer shell and oil and water are probably the most important, together with hydrophobic, van der Waals and electrostatic interactions.

In this second model, the total energy of a core@shell nanoparticle (close to an interface already populated by some NPs) as a function of its position relative to the interface can be written as the sum of several terms. E(z)= E :

$$E = E_W + E_A + E_R + E_{HB} + E_O + E_P \qquad \text{(S.E2)}$$

Where E_W is the same as in equation S.E1, E_A is the van der Waals interaction, E_R is a double layer electrostatic repulsion, E_{HB} is the attractive hydrophobic interaction, E_O is the polymer repulsive osmotic term and E_P is the interaction of the polymer shell with the solvent and.

In the following, the terms in equation S.E2 are described:

1. (E_A + E_R) We describe the interfacial NP interactions on the waterside in terms of the DLVO theory, which accounts for a van der Waals (VdW) E_A interaction and a double layer electrostatic repulsion $E_R = E_R^{i} + E_R^{ii}$ between a NP in the sub-phase and the interface.[8] Here we consider the particular but

representative case shown in **Fig. S.5A**. In the following calculations both the NP-bare interface and NP-adsorbed NP interactions are taken into account. The latter interactions describe the interaction between a NP in the sub-phase at a generic distance from the interface and the interfacially trapped NPs (see **Fig S5A**).

In a first approximation, we estimate the interactions in a semi dilute interfacial regime considering the interactions of a NP in the subphase with the first three neighbor NPs trapped at the interface (arranged in hexagonal lattice). The distance between the NP in the subphase and the adsorbed NPs is supposed to be the same (= D_2, see **Fig S5A**). Note that the VdW term is attractive for NP-adsorbed NPs interactions, whilst is repulsive for the NP- bare interface interaction.

$$E_A = -\frac{A_{H,1}R}{6D_1} - 3\frac{A_{H,2}R}{12D_2} \qquad \text{(S.E3)}$$

Where D_1 , D_2 and are the distances defined in **Fig. S5A**, $A_{H,1}$ (< 0) is the Hamaker constant describing the NP-bare interface interaction and $A_{H,2}$ (> 0) is the Hamaker constant describing the NP-adsorbed NPs interactions.

The electrostatic term is repulsive for both NP-bare interface (E_R^i) and NP-adsorbed NPs (E_R^{ii}) interactions

$$E_R^i = 16\varepsilon R\left(\frac{kT}{e}\right)^2 \tanh\left(\frac{e\psi_{NP}}{4kT}\right)\tanh\left(\frac{e\psi_w}{4kT}\right)\exp(-\kappa D_1) \qquad \text{(S.E4a)}$$

$$E_R^{ii} = 3\cdot 64\pi kT \tanh\left(\frac{e\psi_{NP}}{4kT}\right)^2 \left(R\rho_\infty/\kappa^2\right)\exp(-\kappa D_2) \qquad \text{(S.E4b)}$$

Where ε is the dielectric constant, ρ_∞ is number density of ions in solution, e is the electron charge, ψ_{NP} is the electrostatic potential of the NP, ψ_w is the electrostatic potential of the interface and κ^{-1} is the Debye screening length.

2. (E_{HB}) In the framework of the DLVO theory, for gold NPs close to a bare oil-water interface the VdW interaction is repulsive as the electrostatic term. This leads to an infinite energy barrier which theoretically prevents the adsorption of NPs onto the interface. The attractive term for these system is due to the hydrophobic interaction.[9, 10] To describe the hydrophobic interactions at the water-oil interface, we use the same formula applied for silver and gold nanoparticles at the water-oil interface:[9]

$$E_{HB} = -10\wedge\left(\frac{a_{HB}}{2}(\cos\theta + \cos\theta_0) + b_{HB}\right)\frac{R}{D_1} \quad \text{(in Joule units)} \qquad \text{(S.E5)}$$

Where a_{HB} = –8.2 b_{HB} = – 20 are two system specific constants, $\theta = 40°$ is the absolute contact angle and $\theta_0 = 180°$.[9]

3. (E_P) Based on the Flory-Huggins theory an interaction parameter χ_{FH} can be used to describe the solution behavior of the (polymer) shell.[11] In this theory, $\chi_{FH} \approx \Delta\omega/RT$, where $\Delta\omega$ describes the interaction energy between the polymer and the solvent. When the interaction between solvent and polymer is favorable, $\chi_{FH} < 1/2$ ("good solvent"); whilst $\chi_{FH} > 1/2$ in a "poor solvent" condition.

E_P in equation S.E2 represents the polymer shell interaction and it could be written following a recent work of Isa *et al*:[5]

$$E_P = n_1 f_1(\chi_{FH,1}) + n_2 f_2(\chi_{FH,2}),$$
$$f_i / kT = N / \phi\,[(1-\phi)\ln(1-\phi) + \chi_{FH,i}\,\phi(1-\phi)] \qquad \text{(S.E6)}$$

Where n_i are the number of chains in each medium ($n = n_1 + n_2 = 4\pi R^2 / \Sigma = 31$, where R = 10 nm is the radius of the NP core and Σ is the area per chain. In a mushroom Σ is typically 1 m^2/mg), f_i the free energy of the polymer in each medium, N (= ca 100) is the number of monomer in a chain, $\phi = N\,a^3 / V$ (a = 0.5 nm is the size of the persistence length, $V = 4\pi/3n\,[(R+P)^3 - R^3]$ is the available volume in the shell per chain, P = 6 nm is the height of the polymer shell as evaluated by DLS in **Fig. S1**) is the volume fraction of the polymer in the shell (see section S.2).

Moreover in the aqueous phase, the hydration state of water molecules on the polymer has a specific effect on the solution behavior. In this sense, the interaction parameter χ_{FH} in water must account for a specific hydration term χ_H.

4. (E_O) When the shell of the nanoparticle is composed of polymers, a repulsion term due to the osmotic pressure should be accounted. The latter repulsion energy (in a dilute or semi-dilute regime) can be also described as an exponential function:[10]

$$E_{R,P} \approx n_P 36kT \exp(-D_2 / R_G)\,, \qquad \text{(S.E7)}$$

Where n_P is the number of chains contributing to the osmotic pressure, R_G is the radius of gyration of the polymer.[10]

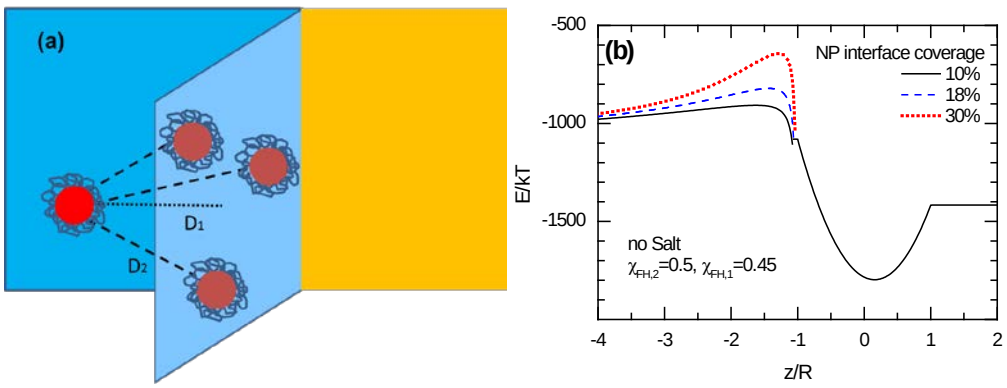

Figure S5. Energy of a single particle as a function of its position relative to the interface calculated from Eq. S.E2-7 for R=10 nm σ_1=1 mN/m, σ_2=1.6 mN/m and γ=7 mN/m (as in the previous model, see the text). The particular case of a particle placed at a generic distance *z* in the water close to a partially populated interface is considered (Fig (a)). Fig (b) shows the effects of NP interface coverage.

Now we use this model to discuss *(i)* the effect of the NP interface coverage (**Fig. S5b**); *(ii)* the experimental observations for the transfer from water to toluene upon increasing salt concentration (**Fig. 5A**), and *(iii)* the effect of changing the interaction parameter χ_{FH} for the transfer from toluene to water (**Fig. 5B**). The total energy (equation S.E2) in **Fig. S5** and **Fig. 5** was calculated using some literature values for the parameters in equations S.E2-7. ε = 7.08 10^{-10} C^2/m, $A_{H,1}$ =–3.9 10^{-20} J , $A_{H,2}$ = 2.5 10^{-19} J,[12] $\chi_{FH,1}$ = 0.45, $\chi_{FH,2}$ =0.5.[13-17] ψ_{NP} = -40 mV, ψ_W = -80 mV.[9, 18] In equation SE.7, we assumed that half of number of the copolymer contribute to the osmotic repulsion $n_P = n/2$.

For the bare toluene-water interface, we choose ρ_∞ = 3 10^{23} m^{-3} and κ= 3 10^7 m. For a salt concentration of 1 mM, ρ_∞ = 6 10^{23} m^{-3} and κ= 1 10^8 m. For a salt concentration 10 mM, ρ_∞ = 6 10^{24} m^{-3} and κ= 3 10^8 m.[10]

In this model the energy plateau values E_1 and E_2 ($z > R$ and $z < -R$ respectively) depend not only on the surface energies as in section S3.1 but also on the interactions between the (polymer) shell and the medium.

Fig. S5B shows the dramatic difference between the interfacial interactions for isolated NP at the bare interface (section S3.1) and in a semidilute interfacial regime. Increasing the NP coverage at the interface, the distance D_2 reduces and the repulsive term E_O and E_R^{ii} increases significantly. The energy barrier calculated using typical value for water-oil interfaces increases from 100 to 400 kT when the coverage increase from 10 to 30%.

An energy barrier in the aqueous medium results from the interplay between the DLVO terms, the hydrophobic interaction and the osmotic pressure. Experimental results based on dynamic interfacial tension data by Kutuzov et al.[19] and Du et al.[4] have already partially discussed such as energy barriers.

Fig. 5A shows how the energy barrier depends strongly on the electrostatic repulsive terms: it increases when ρ_∞ increases, and decreases when κ^{-1} decreases. Note that adding a relative small amount of salt (1 mM) lead to the vanishing of the electrostatic barrier (ca 100 kT).

From the crossing phenomenon viewpoint, increasing salt concentration leads to the transfer from water to toluene as observed in **Fig. 1.**

In **Fig. 5A**, the literature values $\chi_{FH,1}$ = 0.45 and $\chi_{FH,2}$ =0.5 were used.[13-17] Comparing to the model described in S3.1, we observed that the difference in free energy between the two bulk phase is increased from $\Delta E = E_1 - E_2 = -200$ kT to –300 kT.

In **Fig. 5B** the effect of changing the interaction parameter is further investigated. Note that $\chi_{FH,1}$ = 0.45, $\chi_{FH,2}$ =0.5 represent the case when toluene is a "better" solvent than water. Whilst $\chi_{FH,1}$ = 0.55, $\chi_{FH,2}$ =0.45 correspond to the inverse situation when water becomes a better solvent for the copolymer. Note that a difference of the interaction parameter $\Delta\chi_{FH}$ =0.1 lead to a change of 300 kT in the total free energy. Then, we can use the results shown in **Fig.5B** to explain the crossing from toluene to water. As discussed before, for a NP at T ≥ 20°C toluene represents an energy state –300 kT more convenient than water ($E_1 < E_2$). However, for T < 15°C toluene becomes a "poor" solvent and $\chi_{FH,1}$ becomes larger than 1/2 . On the other side, in water at low temperatures, a transition in the hydration state of the PEGylated copolymer could lead to a decrease of the interaction parameter, $\chi_{FH,2} < 1/2$. In this scenario, depicted in **Fig. 5B**, the NP interactions become more favorable in water than in toluene ($E_2 < E_1$), explaining the transfer from water to toluene at low temperatures.

Lastly, adding the polymer free energy on the total energy has also an effect on the minimum of the free energy; *i.e.* the contact angle is shifted towards the medium with lower interaction parameter χ_{FH} (see **Fig. 5B**).

To summarize, in this section a more realistic scenario for the transfer of core@shell NPs is described (see **Fig. S5 and 5**). For a NP radius of 10 nm, we show quantitatively that: *(i)* the NP interfacial coverage has a dramatic effect on the interfacial interactions, *(ii)* the crossing phenomenon from water to toluene happens when the electrostatic barrier (ca 100 kT) vanishes upon the addition of salt (**Fig. 5A)** *(iii)* at low temperatures, the crossing phenomenon from toluene to water is due to a change of the interaction parameter $\Delta\chi_{FH}$ = 0.1 (ΔE = ca 300 kT), which leads to $E_2 < E_1$.

S6 the size effect of nanoparticles on crossing toluene/water interfaces.

Figure S6a shows aqueous dispersions of Au@MEO_2MA_{90}-co-$OEGMA_{10}$ NPs (lower phase) in contact with toluene (upper phase). The particle comprise monodisperse, quasi-spherical gold cores of 32 nm and 48 nm in diameter (labeled on the plastic vials) and the polymer brush shells of about 4 nm thick. **Figure S6b** shows that all the gold nanoparticles attach to the toluene/water interface upon increase of the ionic strength of the aqueous dispersion to 0.15 M. Since the nanoparticles attach to the interfaces between the walls of the plastic vials and the water phase, the whole water phase is enclosed by densely packed gold nanoparticle monolayers, which strongly reflect the light. **Figure S6c** shows that the nanoparticles remain at the toluene/water interfaces after storage at 4 °C overnight.

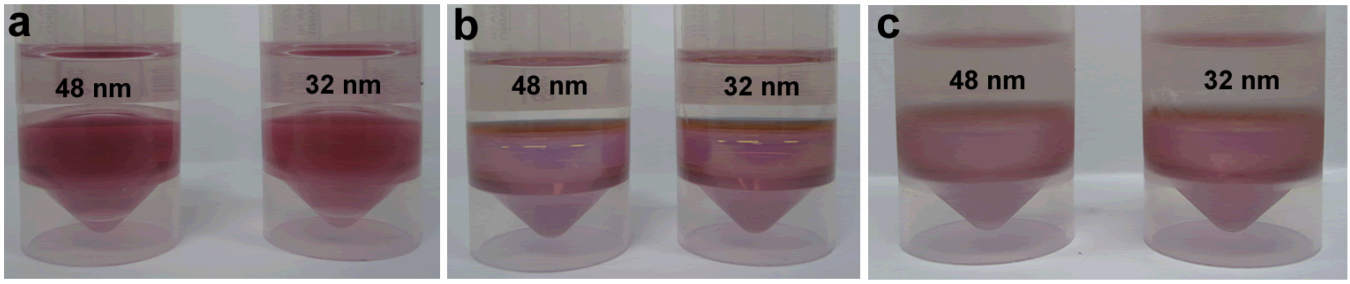

References:

[1] E. W. Edwards, M. Chanana, D. Wang, H. Moehwald, *Angew. Chem.* **2008**, *120*, 326.
[2] J. F. Lutz, . *J Polym Sci Part A: Polym Chem* **2008**, *46*, 3459.
[3] H. Xia, S. Bai, J. Hartmann, D. Wang, *Langmuir* **2010**, *26*, 3585.
[4] K. Du, E. Glogowski, T. Emrick, T. P. Russell, A. D. Dinsmore, *Langmuir* **2010**, *26*, 12518.
[5] L. Isa, E. Amstad, K. Schwenke, E. Del Gado, P. Ilg, M. Kroger, E. Reimhult, *Soft Matter* **2011**, *7*, 7663.
[6] P. Pieranski, *Phys. Rev. Lett.* **1980**, *45*, 569.
[7] A. Stocco, W. Drenckhan, E. Rio, D. Langevin, B. P. Binks, *Soft Matter* **2009**, *5*, 2215.
[8] D. F. Evans, H. Wennerstrom, *The Colloidal Domain*, Wiley-VCH.
[9] X. Lijun, H. Guobin, H. Jiawen, H. Yan, P. Jiangao, L. Yongjun, X. Jiannan, *Phys. Chem. Chem. Phys.* **2009**, *11*, 6490.
[10] J. Israelachvili, *Intermolecular and Surface Forces*, Academic Press, 2nd ed, **1991**.
[11] U. W. Gedde, *Polymer Physics*, Kluwer Academic Publishers, Dordrecht, The Netherlands, **1995**.
[12] T. Kim, K. Lee, M.-S. Gong, S.-W. Joo, *Langmuir* **2005**, *21*, 9524.
[13] Y. C. Bae, J. J. Shim, D. S. Soane, J. M. Prausnitz, *J. Appl. Polym. Sci.* **1993**, *47*, 1193.
[14] F. Doumenc, H. Bodiguel, B. Guerrier, *Eur. Phys. J. E* **2008**, *27*, 3.
[15] A. Eliassi, H. Modarress, G. A. Mansoori, *Journal of Chemical and Engineering Data* **1999**, *44*, 52.
[16] M. Fernández-Berridi, G. MartinGuzmán, J. Iruin, J. Elorza, *Polymer* **1983**, *24*, 417.
[17] C. Ozdemir, A. Guner, *J. Appl. Polym. Sci.* **2006**, *101*, 203.
[18] A. M. Djerdjev, J. K. Beattie, *Phys. Chem. Chem. Phys.* **2008**, *10*, 4843.
[19] S. Kutuzov, J. He, R. Tangirala, T. Emrick, T. P. Russell, A. Boker, *Phys. Chem. Chem. Phys.* **2007**, *9*, 6351.